Journal of Alloys and Compounds 512 (2012) 100–104

Contents lists available at SciVerse ScienceDirect

Journal of Alloys and Compounds

journal homepage: www.elsevier.com/locate/jallcom

Influence of the thermo-chemical conditions on the carbo-chromization process of α-Fe matrices obtained by powder sintering technique

S. Iorga [a], S. Ciuca [a], C. Leuvrey [b], S. Colis [b,*]

[a] Polytechnic University of Bucharest, Splaiul Independentei 313, 77204 Bucharest VI, Romania
[b] Institut de Physique et Chimie des Matériaux de Strasbourg (IPCMS), UMR 7504 CNRS and University of Strasbourg (UDS-ECPM), 23 rue du Loess, BP 43, F-67034 Strasbourg Cedex 2, France

ARTICLE INFO

Article history:
Received 25 July 2011
Received in revised form 6 September 2011
Accepted 6 September 2011
Available online 16 September 2011

Keywords:
Thermochemical treatments
Carburization
Chromization
Powder metallurgy
α-Fe
Scanning electron microscopy
Hardness

ABSTRACT

We report on the superficial layer formation resulting from the carburization followed by chromization of α-Fe samples obtained by powder sintering technique. The carburization and chromization were carried out by thermal diffusion between 880–980 °C and 950–1050 °C in a solid powder mixture of charcoal/$BaCO_3$ and ferrochromium/alumina/NH_4Cl, respectively. The obtained layers were investigated using X-ray diffraction, optical microscopy, Vickers micro-hardness technique and scanning electron microscopy. The results show that the layers are of micrometric size and consist mostly of chromium carbides of different phases. These phases as well as the thickness of the layers are closely related to the treatment temperature used for carburization and to the temperature and Cr initial concentration in the mixture used for chromization. For highly reactive carbo-chromization conditions (high concentration of Cr, and high carburization and chromization temperatures) the superficial layer is constituted of two chromium carbide sub-layers (Cr_3C_2/Cr_7C_3) separated by a sharp interface. The thickness and hardness of the coating layer reached 45 μm and 2300 HV, respectively. Such coating could be used for tools that have to be abrasion and oxygen resistant at high temperatures.

1. Introduction

The search for new coatings to improve the resistance of materials to different mechanical stresses has always been a challenge in materials science [1,2]. Among these materials, Fe–Cr–C alloys are used in severe conditions to prevent erosion where large abrasion resistance is necessary [3–5]. Although their hardness is lower than that of vanadium or tungsten carbides, chromium carbides obtained during the preparation of Fe–Cr–C present a much better high-temperature oxidation resistance up to 700 °C [6]. In many cases, obtaining Fe–Cr–C coatings was achieved by diffusing Cr into Fe–C or low C content steel [7]. Due to the limited diffusivity of chromium at low temperatures, the conventional chromization processes are usually carried out at temperatures around 1000 °C during 6–10 h [7,8]. Studies have revealed that the layers obtained by carburization followed by chromization consisted mostly of carbides with the following crystallographic structures: $M_{23}C_6$, M_7C_3, and M_3C_2 [4,5,7,9]. However, the Fe–Cr–C layer properties depend strongly upon the process and the parameters (such as temperature, time, and atmosphere) of the thermochemical treatment.

The aim of this paper is to determine the phase and composition of Fe–Cr–C layers following the independent carburization and chromization of α-Fe samples obtained by powder metallurgy techniques. This process is studied on samples containing different amounts of C and Cr, obtained by thermal diffusion at different temperatures and using different concentrations of Cr in the starting mixture used as Cr source. The microstructure, chemical composition, and hardness of carbo-chromized layers are investigated.

2. Experimental details

All samples were made by powder metallurgy technique. α-Fe powder was pressed at 735 MPa and then sintered at 1000 °C for 4 h. The obtained samples are cylinders of 16 mm in diameter and 11 mm in height. The sample porosity was estimated from the difference between the theoretical and the experimental densities between 8 and 10%. The carburization treatment was performed in solid environment by placing the Fe sintered sample in a crucible filled with a powder mixture of 80% charcoal (as carbon source) and 20% of $BaCO_3$ (as activator). The treatment temperature and time were of 880 °C for 4 h and 980 °C for 12 h which resulted in samples with a low and high carburization depth. The carburized samples were further chromized in solid environment, using a mixture of ferrochromium powder (as chromium source), ammonium chloride powder (as activator) and alumina powder

* Corresponding author.
E-mail address: colis@ipcms.u-strasbg.fr (S. Colis).

0925-8388/$ – see front matter © 2011 Elsevier B.V. All rights reserved.
doi:10.1016/j.jallcom.2011.09.030

Table 1
Sample preparation conditions summarizing the mixture, temperature and time used for carburization and chromization. The carburization mixture was 80% charcoal + 20% $BaCO_3$ for all samples. The letters *l* and *h* in the sample names stand for *low* and *high* content, respectively.

Sample	Carb. temp.	Carb. time	Chrom. temp.	Chrom. time	Chrom. mixture
S1 (*h***C***h***Cr**)	980 °C	12 h	1050 °C	12 h	21% Al_2O_3 + 3% NH_4Cl + 76% ferrochromium
S2 (*h***C***l***Cr**)	980 °C	12 h	950 °C	6 h	72% Al_2O_3 + 3% NH_4Cl + 25% ferrochromium
S3 (*l***C***h***Cr**)	880 °C	4 h	1050 °C	12 h	21% Al_2O_3 + 3% NH_4Cl + 76% ferrochromium
S4 (*l***C***l***Cr**)	880 °C	4 h	950 °C	6 h	72% Al_2O_3 + 3% NH_4Cl + 25% ferrochromium

(introduced in the composition mixture to prevent the sintering of ferrochromium particles and their bonding to the sample surface) [9,10]. The mixture used for chromization had different proportions of ferrochromium (76 and 25%) and alumina (21 and 72%), while the NH_4Cl (3%) remained constant. Both carburization and chromization were carried out in a crucible made of refractory steel of 120 mm in diameter and 130 mm in height. The treatment temperature and time for chromization were of 950 °C for 6 h and 1050 °C for 12 h. Consequently, a low and high amount of chromium could be inserted in the carburized sample.

By combining these sample preparation conditions, due to diffusion phenomena, four samples were obtained (S1–S4) containing different contents of C and Cr. The sample preparation conditions for each sample are summarized in Table 1. Note that other samples prepared in intermediate synthesis conditions showed results in agreement with the conclusions drawn from the study of the S1–S4 samples. For this reason and since they do not provide new additional information in support of the presented phenomena they will not be presented here and only the extreme cases (S1–S4 samples) will be discussed.

The characterization of the carbo-chromized layers was performed on cross-section specimens prepared by polishing with 1 μm diamond paste and etched with Murakami reagent.

The cross-sectional microstructure and morphology of the coatings were observed using an Epytip optical microscope and a JEOL JSM-6700F scanning electron microscope (SEM). The SEM microscope is equipped with an energy dispersive X-ray spectroscopy (EDS) analyzer that was used to determine the chemical composition of the layers. The elemental mapping was obtained by analyzing the K lines of each element of the EDS spectra recorded in each point of the image.

The Vickers hardness across the coating was measured on a Hanneman micro-hardness tester equipped with a four-sided diamond pyramidal indenter. A load force of 50 mN and a dwelling time of 10 s were applied during the tests.

The crystalline structure of the coatings was investigated by X-ray diffraction (XRD). The spectra were recorded in $\theta - 2\theta$ mode using a Simens D5000 diffractometer operating with Cu Kα radiation (λ = 1.54056 Å) at 35 kV and 25 mA.

3. Results and discussion

The first information on the Fe–Cr–C layers was obtained by optical microscopy. The cross-section images of the four samples are shown in Fig. 1. For visibility reasons the samples were etched with Murakami reagent. The images highlight the formation of carbo-chromized layers on the sample surface. All samples show a porosity probably due to an insufficient sintering temperature and/or time of the Fe samples. This can lead to inhomogeneities and to variations of the Fe–Cr–C thickness at the sample surface. Indeed, all samples show the formation of a coating layer with rather inhomogeneous thickness. It can be also seen that at the interface with the Fe substrate, the coating layer tends to fill the surface porosity leading to columnar-like insertions (well visible in

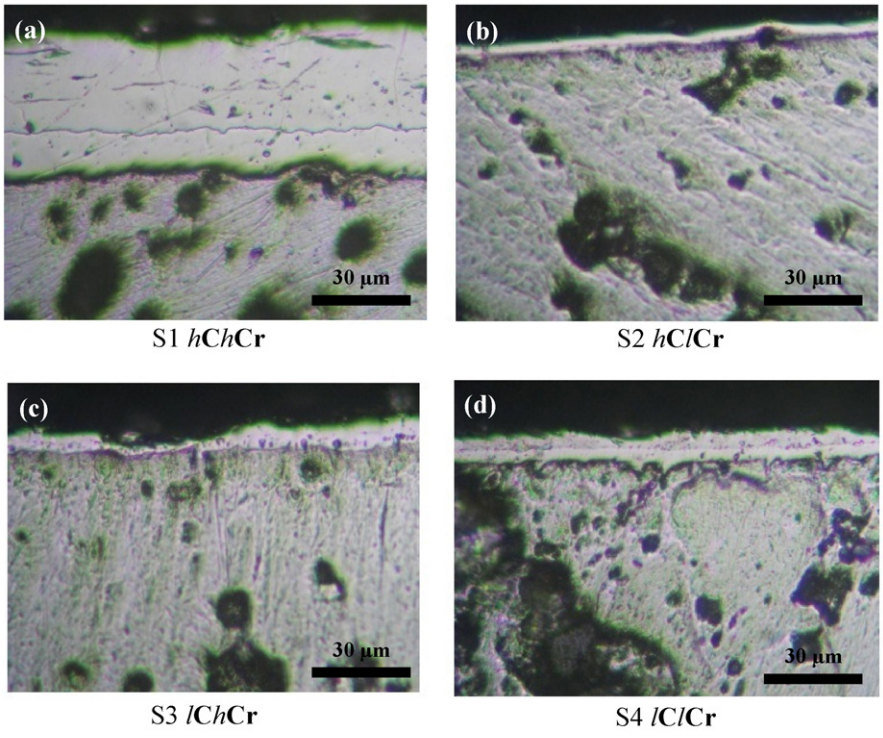

Fig. 1. Optical microscopy cross-section images of (a) S1 ***h*C*h*Cr**, (b) S2 ***h*C*l*Cr**, (c) S3 ***l*C*h*Cr** and (d) S4 ***l*C*l*Cr** samples.

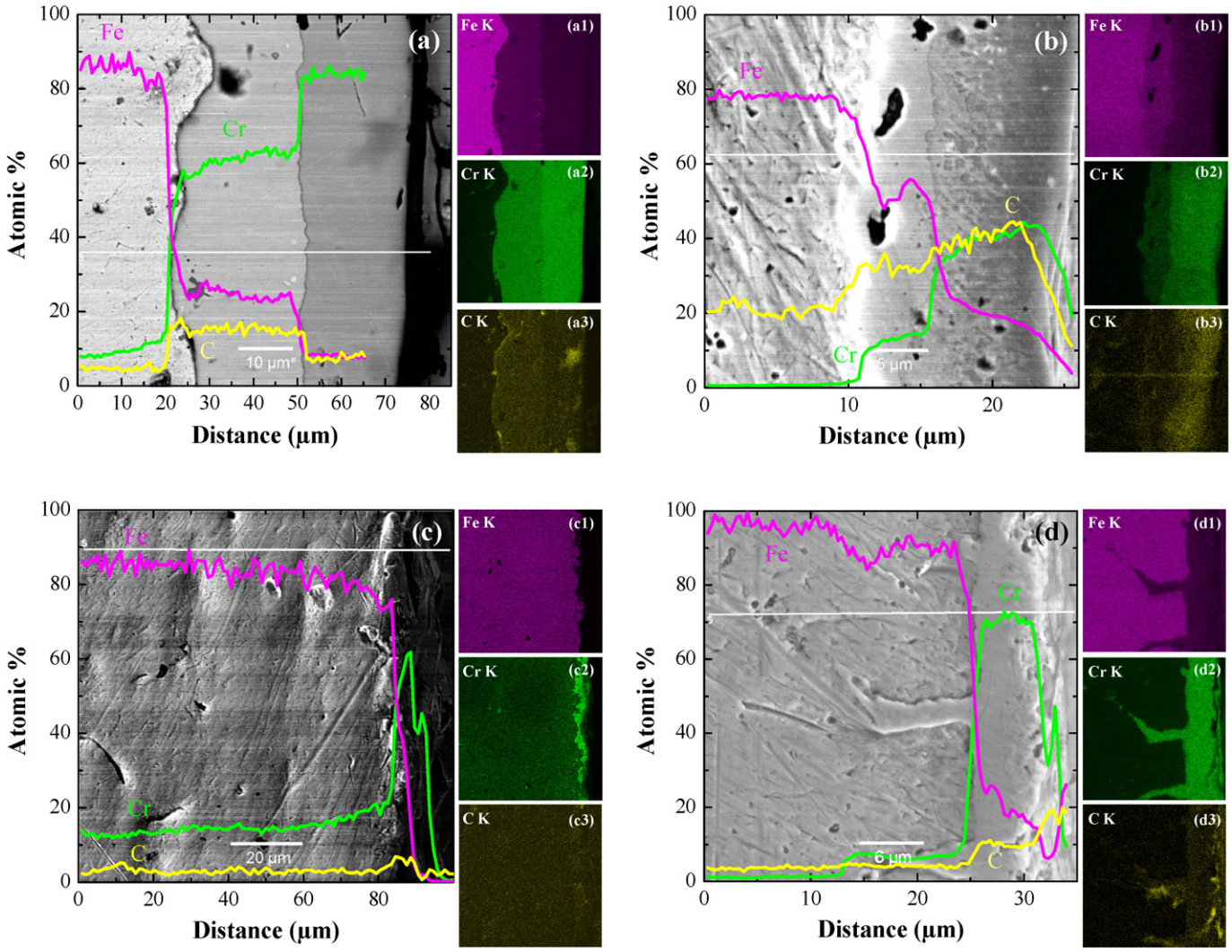

Fig. 2. Scanning electron microscopy cross-section images of (a) S1 ***h*ChCr**, (b) S2 ***h*ClCr**, (c) S3 ***l*ChCr** and (d) S4 ***l*ClCr** samples. The concentration profile of Fe, Cr, and C recorded using EDS measurements along the white line was superimposed to the figure. The mapping of the same chemical elements is also shown on the right side of each figure [(a–d)1 to (a–d)3].

Fig. 1d) in the Fe surface. The thickness of the coating layer ranges from about 8 to 10 μm in samples S2 ***h*ClCr**, S3 ***l*ChCr** and S4 ***l*ClCr**, and increases drastically up to about 45 μm in sample S1 ***h*ChCr**. It is interesting to note that the obtention of a thick coating layer requires a large amount of both C and Cr, and seems independent on the "infinite" source of Fe beneath. This suggests that Fe from the substrate presents a limited role in the formation, and therefore, in the thickness and the mechanic properties of the coating layer. Another interesting observation is that in sample S1 ***h*ChCr**, the coating layer seems composed of two layers, separated by a sharp interface (Fig. 1a). The external layer is about 30 μm thick, while the inner layer has about 15 μm. Although the total thickness of the coating is much smaller, a similar "bilayer" can be also observed in sample S4 (***l*ClCr**). These two layers are probably constituted of carbide phases with different Fe (if any), Cr and C concentrations. Lee and Duh [7] attributed the inner and outer layers to $(Cr,Fe)_{23}C_6$ and $(Cr,Fe)_2N_{1-x}$ phases, respectively, thus suggesting that C can be absent from the sample surface. Other works, as the one of Fan et al. [5], report the existence of $(Cr,Fe)_{23}C_6$ with traces of $(Cr,Fe)_7C_3$. This situation can be reversed in the case of Fe–Cr–C eutectic composites where $(Cr,Fe)_7C_3$ is the major phase and $(Cr,Fe)_{23}C_6$ is the minor one [11]. This suggests that the preparation conditions influence strongly on the phases present in the coating layer, and further, on its mechanical properties. Therefore, in order to have a closer look to the morphology of the coating layer and check the chemical composition along its thickness, SEM observations have been carried out.

Fig. 2 shows SEM cross-section images of the coating layer for the four samples (S1–S4). These images confirm the observations made by optical microscopy. The thickness and the morphology of the layers are even better evidenced, as well as the two layers that form the coating layer. Fig. 2 shows also the distribution of Fe, Cr, and C along the coating layer thickness (a–d) and a mapping of the same elements on the SEM image [(a–d)1 to (a–d)3]. The presence of O, N, Al and Ba has also been checked (not shown here) but no traces (i.e. contrast variation) could be evidenced. This let us think that no nitride layer is present in our samples as this was the case in other studies [7] and that the activators do not pollute the resulting coating layer. Although Cr, Fe and C could be evidenced in the coating layer, we cannot conclude on the nature of the carbide phases that constitute the coating. This is mainly due to the poor quantification (using EDS) of light chemical elements such as C.

The mapping of the chemical elements allows, however, few hypothesis on the nature of the coating. The sample S1 ***h*ChCr** presents the layer with the largest thickness of the coating layer. During carburization, a large amount of carbon was inserted in the

matrix because of the large temperature and time used for this process. Following this carburization, the chromization was conducted in a high Cr concentration, at high temperature and during a long time. A large amount of Cr is expected to diffuse in the carburized sample and interacts with the C present at the sample surface resulting in a thick coating layer. It is important to point out that, as already observed by optical microscopy, the mapping of the chemical elements does not show a continuous gradient of C and Cr from the surface towards the inside of the sample but presents a stepped variation. This suggests that Cr is attracted by C (existing under ferrite and cementite forms) and leads to Cr rich phases which limit further the diffusion of Cr to the inside of the sample. It appears therefore that Cr rich phases are located at the surface while phases with lower Cr content are located deeper below the surface. Moreover, due to the high temperature used during chromization, the sample can undergo a C migration towards the sample surface. This favors the blocking of Cr diffusion deep in the sample and the formation of chromium carbides with a phase depending on the local Cr/C ratio. Within this model, one can therefore easily understand that the external layers are formed of Cr rich carbides and that the interface between two chromium carbide phases is sharp and perpendicular to the gradient of concentration of Cr and C (i.e. parallel to the sample surface). This is exactly what is observed in Fig. 2. Many studies reporting on the chromization of Fe–C matrices show that the formed carbides are mostly of $Cr_{23}C_6$, Cr_7C_3 and Cr_3C_2 type. Since the formation enthalpy of $Cr_{23}C_6$ (Cr/C ratio of 3.83) is larger than that of Cr_7C_3 (Cr/C ratio of 2.33), which is larger than that of Cr_3C_2 (Cr/C ratio of 1.5) [12], the two carbides layers observed in our samples are either $Cr_{23}C_6$ and Cr_7C_3, or Cr_7C_3 and Cr_3C_2. These phases may contain some Fe, since a stepped profile with an increasing Fe concentration is observed in each layer while moving from the surface towards the sample core (Fig. 2a and a1). The presence of carbide phases containing Fe [generally noted $(Cr,Fe)_xC_y$] has already been suggested by Lee and Duh [7].

Compared to the S1 ***h*ChCr** sample, the S2 ***h*C*l*Cr** one is supposed to contain the same amount of C since the carburization was carried out in the same conditions for the two samples. Nevertheless, the chromium carbide coating has a small thickness of only 10 μm while below the coating layer the concentration of C is small as in the rest of the sample. This suggests that once the chromium carbide layers are formed, the migration of atoms inside the sample leads to a low C concentration inside the inner part of the carburized layer. A similar behavior is observed for the S3 ***l*Ch*l*Cr** sample (Fig. 2c). Due to the low content of C in the superficial layer (i.e. small thickness), only a small amount of Cr is trapped at the surface to form a chromium carbide coating layer. This is particularly evidenced by the thin and sometimes discontinuous character of the coating layer and by the Fe–Cr solid solution expected below this layer. The existence of the Fe–Cr solid solution is consistent with the large concentration of Fe and Cr in the core of the sample (Fig. 2c). In the case of sample S4 ***l*C*l*Cr**, the coating layer is still thin (about 10 μm) and still composed of two sub-layers corresponding to two carbide phases (Fig. 2d).

These observations clearly indicate that a thick layer of carbide coating requires both a large amount of C and Cr in the sample. If one amount is much larger than the other, the carbide layer will be thin. The sample either will have a small C concentration if the concentration of C is much larger than the one of Cr, or will form a solid solution if the concentration of Cr is much larger than the one of C. With respect to most studies focused on the chromization of steel to obtain a hardfacing layer, the simple two-step method of thermal diffusion where carburization and chromization are performed independently, allows to obtain thick coatings which may resist longer to corrosion or mechanical abrasion.

The Vickers micro-hardness measurements performed on the cross-section coating layer confirmed the existence of carbide

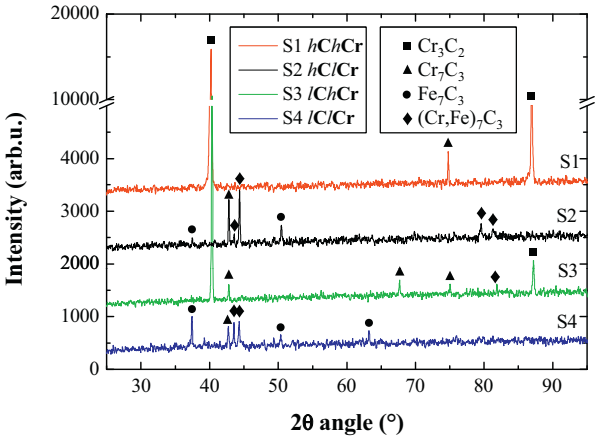

Fig. 3. X-ray diffraction patterns recorded on the S1 ***h*ChCr**, S2 ***h*C*l*Cr**, S3 ***l*Ch*l*Cr** and S4 ***l*C*l*Cr** samples.

phases at the surface of our samples. Indeed, all samples present values of the hardness larger than 1400 HV [13,14]. A fine hardness analysis along the growth direction showed a stepped decrease when moving the indenter from the surface towards the inner part of the sample. In the case of sample S1 ***h*ChCr**, the hardnesses of the outer and inner layers are about 2300 and 1780 HV, while the hardness of the α-Fe matrix (or Fe–Cr solid solution) is only about 170–230 HV. This large values of hardness are compatible with the Cr_7C_3 (outer layer) [14] and Cr_3C_2 or $Cr_{23}C_6$ (inner layer). The distance for which the large hardness remained constant corresponds well to the thicknesses of the two sub-layers as these were measured from optical and SEM microscopy.

In order to elucidate the nature of the phases contained in the coating layer, XRD patterns were recorded on the S1–S4 samples and shown in Fig. 3. It can be easily seen that the samples containing a large amount of Cr (S1 ***h*ChCr** and S3 ***l*Ch*l*Cr**), present both Cr_3C_2 and Cr_7C_3 phases. The fact that only few peaks are observed for each phase suggests a texture effect. In contrast, when the Cr concentration is reduced (S2 ***h*C*l*Cr** and S4 ***l*C*l*Cr**), the carbide layers incorporate as well Fe and lead to the appearance of $(Cr,Fe)_7C_3$ and Fe_7C_3. No traces of $Cr_{23}C_6$ phase could be detected in any of the samples. This let us think that although $Cr_{23}C_6$ has the most negative enthalpy of formation with respect to the other chromium carbides [12], the Cr concentration with respect to C (i.e. the Cr/C ratio) in the coating layer never gets sufficiently high to form $Cr_{23}C_6$ as the diffusion of Cr occurs too rapidly. This was checked on a sample in which a Cr layer has been electro-deposited on a carburized α-Fe sample (results not shown here). The treatment temperature used to diffuse Cr inside the sample leaded to a high Cr/C ratio at the surface sample, and therefore, to the presence of the $Cr_{23}C_6$ phase. A similar phenomenon is observed when coating low carbon content steel samples [7,15]. The $Cr_{23}C_6$ phase is easily obtained in this case due to the low carbon content of steel, which leads rapidly to high enough ratios of Cr/C during chromization. It is also interesting to point out that using the same preparation technique (pack cementation), Lee and Duh [7] reported the existence of a $(Cr,Fe)_2N_{1-x}$ phase at the coating surface. The presence of nitrogen at the film surface was confirmed in their case by EDS analyzes. Although some diffraction peaks from our patterns could correspond to $(Cr,Fe)_2N_{1-x}$, this possibility was excluded in our work since no nitrogen was detected at the sample surface (EDS analysis). Moreover, these peaks do not appear systematically in all patterns although the potential contamination with N is similar for all samples. It is therefore reasonably to assume that our coating layer obtained in the sample S1 ***h*ChCr** is composed of a

Cr_3C_2/Cr_7C_3 bilayer. The situation is more complex for low Cr concentration coatings. In this case only traces of Cr_7C_3 subsist in the coating as this phase is replaced by mixed chromium and iron carbide ($(Cr,Fe)_7C_3$) and iron carbide (Fe_7C_3). As a consequence, the hardness of the coating layer decreases down to 1400 HV.

4. Conclusion

α-Fe samples obtained by powder metallurgy techniques were sequentially carburized and chromized using different treatment conditions. This led to coating layers with variable contents of Cr and C. When the amount of Cr and C that diffuses at the sample surface is large, the coating layer is mostly constituted of Cr_3C_2/Cr_7C_3 bilayers. In contrast, when the C and/or Cr content is low, the coating layer is mainly constituted of $(Cr,Fe)_7C_3$ and Fe_7C_3. This simple technique allowed to obtain thick coating layers of about 45 μm and presenting a hardness as high as 2300 HV. These layers are expected to have longer lifetimes and resist better to highly abrasive and corrosive working conditions. Moreover, our study demonstrated the possibility to coat sintered samples obtained by powder metallurgy that would be otherwise difficult to manufacture by more classic cutting or milling techniques.

Acknowledgements

This work has been supported by the Sectoral Operational Programme Human Resources Development 2007–2013 of the Romanian Ministry of Labor, Family and Social Protection through the Financial Agreement POSDRU/88/1.5/S/60203.

References

[1] K.H. Zum Gahr, G.T. Eldis, Wear 64 (1980) 175.
[2] C.P. Tabrett, I.R. Share, Wear 203–204 (1997) 206.
[3] Q. Wang, X. Li, Weld. J. 89 (2010) 133S.
[4] A. Wiengmoon, T. Chairuangsri, A. Brown, R. Brydson, D.V. Edmonds, J.T.H. Pearce, Acta Mater. 53 (2005) 4143.
[5] C. Fan, M.C. Chen, C.M. Chang, W. Wu, Surf. Coat. Technol. 201 (2006) 908.
[6] D.Y. Wang, K.W. Weng, C.L. Chang, W.Y. Ho, Surf. Coat. Technol. 120–121 (1999) 622.
[7] J.W. Lee, J.G. Duh, Surf. Coat. Technol. 177–178 (2004) 525.
[8] Z.B. Wang, J. Lu, K. Lu, Acta Mater. 53 (2005) 2081.
[9] C.Y. Wei, F.S. Chen, Mater. Chem. Phys. 91 (2005) 192.
[10] J.W. Lee, J.G. Duh, S.Y. Tsai, Surf. Coat. Technol. 153 (2002) 59.
[11] L. Lu, H. Soda, A. McLean, Mater. Sci. Eng. A 347 (2003) 214.
[12] M. Detroye, F. Reniers, C. Buess-Herman, J. Vereecken, Appl. Surf. Sci. 120 (1997) 85.
[13] F.S. Chen, P.Y. Lee, M.C. Yeh, Mater. Chem. Phys. 53 (1998) 19.
[14] R.C. Jongbloed, Mater. Sci. Forum 163–165 (1994) 611.
[15] A.J. Perry, E. Horvath, J. Mater. Sci. 13 (1978) 1303.